

Chiral Discrimination of Camphorquinone Enantiomers by Cyclodextrins: A Spectroscopic and Photophysical Study[†]

Pietro Bortolus,* Giancarlo Marconi, and Sandra Monti

Istituto di Fotochimica e Radiazioni d'Alta Energia, CNR, Area della Ricerca, Via Piero Gobetti 101, 40129 Bologna, Italy

Bernd Mayer

Institut für Theoretische Chemie und Molekulare Strukturbiologie, University of Vienna, Althanstrasse 14, 1090 Vienna, Austria

Received: June 5, 2001; In Final Form: October 4, 2001

The complexation of (1*R*)-(–)-camphorquinone and (1*S*)-(+)–camphorquinone with α -, β -, and γ -cyclodextrins (CD) is elucidated by a combination of spectroscopic techniques and theoretical methods applying a dynamic Monte Carlo procedure. The absorption, induced circular dichroism (icd), luminescence, and transient triplet–triplet absorption properties of the two enantiomers are modified by the CDs in agreement with the formation of 2:1 host/guest complexes with α -CD and 1:1 complexes with β - and γ -CD. The equilibrium constants and, in part, the triplet lifetimes indicate a distinct chiral discrimination of cyclodextrins toward the two camphorquinone enantiomers. These results were in addition supported by conformational calculations and theoretical interpretation of icd spectra, which also provided detailed structural data on the complexes.

Introduction

Cyclodextrins (CDs) are naturally occurring cyclic oligosaccharides consisting of six (α -cyclodextrin), seven (β -), and eight (γ -) D-glucopyranose units. Interest in these compounds arises from the fact that, in aqueous solution, they act as host molecules in the formation of inclusion complexes with a wide variety of organic and inorganic compounds.¹ The CDs exist as a single enantiomer, so that, when they form inclusion complexes with optically inactive compounds, an induced optical activity is observed.² When the CDs interact with a racemic guest, the formation of diastereoisomeric complexes of differing thermodynamic stability can occur. The wide use of the CDs as chiral selectors in the chromatographic techniques (HPLC and GLC) and capillary electrophoresis is based on the above-reported property of cyclodextrins.³

Moreover, in some cases, the cyclodextrins act as asymmetric keyholes in host–guest interaction. The formation of a chiral pyrene dimer in the large cavity of γ -CD has been inferred from the strong left-handed circularly polarized excimer fluorescence,⁴ whereas for 4-helicene in the γ -CD cavity and 1,1'-binaphthalene in the β -CD cavity, the formation of chiral dimers has been deduced from the sign of the induced circular dichroism.⁵

Despite the considerable importance of chiral recognition, only scarce data on the free energy difference between CD complexes involving enantiomeric couples of guests are reported in the literature.^{6–14} Chiral discrimination by modified cyclodextrin is reviewed in ref 15.

In the present work, we addressed the problem of the chiral discrimination of cyclodextrins toward (1*R*)-(–)-camphorquinone (RCQ) and (1*S*)-(+)–camphorquinone (SCQ) by a combina-

tion of spectroscopic techniques and theoretical methods applying a dynamic Monte Carlo (DMC) procedure, which provided interesting results with dimethoxybenzenes,^{16a} naphthyl-ethanols,^{16b} and methyl- and phenyl- substituted phenols.¹⁷ The absorption, induced circular dichroism (icd), luminescence, and transient triplet–triplet absorption characteristics of the complexes of α -, β -, γ -, and dimethyl- β -CD with the enantiomeric camphorquinones are reported. The recovered equilibrium constants indicate that α -CD is the best host for chiral recognition of the above guests.

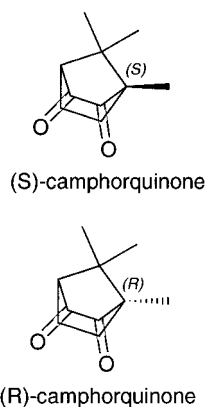
Experimental Section

RCQ and SCQ (Aldrich 99%; Chart 1) and cyclodextrins (α - and β -CD, Serva, γ - and heptakis(2,6-di-*O*-methyl)- β -CD, Aldrich) were used as received. Water was purified by passage through a Millipore MilliQ system. For the emission experiments, stock solutions of enantiomeric camphorquinones were prepared just before the measurements by direct dissolution in water of a weighed amount of the enantiomer ($c \approx 1.5 \times 10^{-3}$ M). When studying the complexation with β -, heptakis(2,6-di-*O*-methyl)- β -, or γ -CD, the highest required amount of CD was added to 3 mL of this stock solution. After filtration through a Millipore filter, the measurement was carried out; this solution was successively diluted with the stock to carry out the experiments with lower [CD]. The solutions containing [α -CD] $> 10^{-2}$ M become cloudy on standing (5–10 min) owing to the precipitation of the inclusion complex. To avoid the complications arising from the precipitation of the complex, each fluorescence and icd spectrum in the presence of [α -CD] $> 10^{-2}$ M was obtained by recording the pertinent property of the stock solution in the presence of the proper weighted amount of dextrin. For solutions containing [α -CD] $< 10^{-2}$ M, the same procedure above-described for the other dextrins was adopted. The concentration of RCQ and SCQ in the absorbance measure-

[†] Paper presented in part at the XVIII IUPAC Symposium on Photochemistry, Dresden, Germany, July 22–27, 2000.

* To whom correspondence should be addressed. Fax: +39 049 641925. E-mail: monti@frae.bo.cnr.it.

CHART 1



ments carried out to estimate the association constants with α -CD was ca. 2×10^{-3} M, and the measurements were done in a 40 mm thick cell. To determine the association constants, titration experiments were also performed measuring the induced circular dichroism. Typically a number of 10–13 concentrations of α -CD as titrant were used. In this case, the guest concentration was about 4.6×10^{-3} M. The computer program Hyperquad2000, distributed by Peters Gans,¹⁸ was used for the calculation.

UV–vis absorption spectra were recorded on a Perkin-Elmer 320 spectrophotometer. The circular dichroism spectra were obtained with a Jasco J-715 dichrograph, and uncorrected luminescence emission spectra were obtained on a Perkin-Elmer MPF 44. All experiments were carried out in cells thermostated at 295 ± 1 °C. Deoxygenation of the solutions in emission experiments was carried out by bubbling nitrogen. The fluorescence quantum yield of CQ enantiomers in aqueous solutions was determined by comparison with equally absorbing acetonitrile solutions (see later). No effect of dissolved oxygen was observed.

Triplet–triplet absorption spectroscopy was carried out by using a laser flash photolysis system that utilizes a Continuum Nd:YAG Surelite II-10 laser, running at 10 Hz and equipped with an optical parametric oscillator (OPO). The selected excitation wavelength was 460 nm, an isosbetic point of the CQ-CD mixtures. A single pulse, typically with energy ≤ 5 mJ and duration of ~ 5 ns, was used to excite the sample. The detection system and the geometric details of the excitation/analysis setup were similar to those described earlier.¹⁹ The constance of the pulse energy was monitored at each laser shot by using a beam splitter and a pyroelectric energy meter (Laser Precision Rj7100). The mean incident power was measured at 10 Hz, by means of a Scientech 365 photocalorimeter, with the head located at the sample cell position. Oxygen was removed from the solutions by Ar bubbling.

Theoretical Methods

Low energy complex geometries were searched by applying a DMC routine, including solvation effects. The method, which combines the potential energies calculated by a force field (MM3) and the free energies of solvation derived from a continuum approximation, proved to give valuable structural results for many CD complexes in aqueous environments. Details of the computational protocol are described extensively in ref 16a–c. A further restriction in the choice of the most reliable structure of the computed complexes was provided by the comparison of the theoretically expected and experimentally observed icd spectrum. Generally, the induction of optical

activity by a chiral medium is described by three terms, known as one-electron, dipole–dipole (d–d), and electric–magnetic interaction ($m-\mu$) mechanism. The first mechanism derives from the interaction of the electric and magnetic transition dipole moments located in different states of the same chromophore and turns out to give a small contribution in case of state mixing because of the electrostatic field of the macrocycle. The second mechanism, d–d, is particularly suited to describe the icd of guests with low-lying allowed π, π^* states and has been widely utilized, in the approximate form, using the polarizability of the CD states,²⁰ to calculate the icd of many aromatic compounds included in cyclodextrins.^{16,17} The third mechanism, $m-\mu$, can be very important for symmetry-forbidden or weakly allowed n, π^* transitions and has been used to reproduce adequately the circular dichroism of carbonyls²⁰ and peptides.²¹ According to Tinoco,²² this term is expressed by

$$R_{0a}(m-\mu) = -2 \sum_{j \neq i} \sum_{b \neq a} \text{Im} \left[V_{ia0, j0b} \left(\frac{\mu_{i0a} m_{j0b} \nu_a + \mu_{j0b} m_{i0a} \nu_b}{h(\nu_b^2 - \nu_a^2)} \right) \right] \quad (1)$$

where

$$V_{ia0, j0b} = \mu_{ia0} \cdot \mathbf{T}_{ij} \cdot \mu_{j0b} \quad (2)$$

and

$$\mathbf{T}_{ij} = \left[1 - \frac{3\mathbf{R}_{ij}\mathbf{R}_{ij}}{R_{ij}^2} \right] \frac{1}{R_{ij}^3} \quad (3)$$

In eq 1, m and μ stand for the magnetic transition dipole moment of the guest and electric transition dipole moment of the macrocycle, respectively, h stands for Planck's constant, and Im stands for the imaginary part. The sums extend over all the excited states a and b , having a frequency of ν_a and ν_b , and over the bonds i and j of the chromophore and macrocycle, respectively. The geometrical factor V of eq 2 contains \mathbf{T}_{ij} , representing the dipole interaction tensor, a direct function of the distance \mathbf{R}_{ij} between the bonds i and j (eq 3). Although the transition dipole moment of the macrocycle lies at high energies (> 8 eV), in the present case, it was found that the terms arising from eq 1 are larger by 2 orders of magnitude with respect to those deriving from the d–d terms.

In the present work, the energies and electric dipole moments were calculated by using the ZINDO/S program included in the Hyperchem package, whereas the magnetic moments in eq 1 were computed within the complete angular momentum operator framework.²³

Results and Discussion

Absorption, Induced Circular Dichroism, and Emission Spectra. The UV–vis absorption spectrum of camphorquinone exhibits two bands attributed to two n, π^* transitions.^{24,25} The spectrum of the two enantiomers is identical, as expected. The long-wavelength absorption band in water is peaked at 453 nm, blue shifted with respect to the maximum in acetonitrile (465 nm), and in cyclohexane (478 nm), in agreement with the n, π^* character of the transition. Figure 1 shows the absorption spectrum of RCQ in water and the effect of the addition of α -, β -, and γ -CD (the effect of dimethyl- β -CD, not shown for sake of clarity, is similar to that of β -CD). Both the long- ($\lambda_{\text{max}} = 453$ nm and $\epsilon = 37 \text{ M}^{-1} \text{ cm}^{-1}$) and the short-wavelength absorption bands are affected by the presence of cyclodextrins

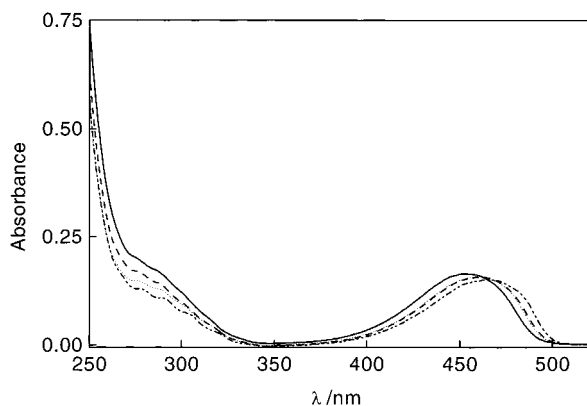


Figure 1. Absorption spectrum of RCQ ($c = 4.52 \times 10^{-3}$ M) in water (—), in the presence of 2.1×10^{-2} M α -CD (---), 1.05×10^{-2} M β -CD (···), and 2.15×10^{-2} M γ -CD (-·-·-); cell path 1 cm, $T = 295$ K.

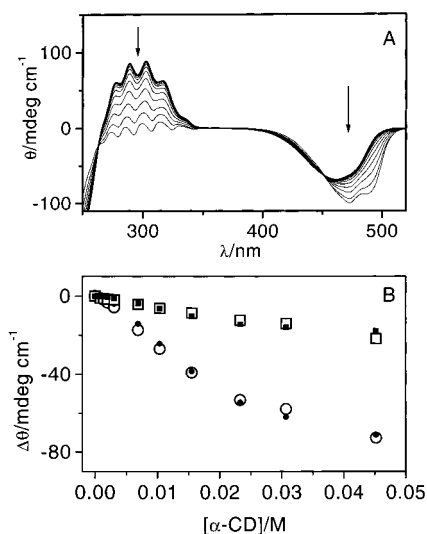


Figure 2. (A) Circular dichroism spectra of RCQ ($c = 4.55 \times 10^{-3}$ M) in water (—) and in the presence of increasing concentrations of α -CD (—); $[\alpha\text{-CD}] = 6.1 \times 10^{-4}$, 9.1×10^{-4} , 1.36×10^{-3} , 2.05×10^{-3} , 3.07×10^{-3} , 4.6×10^{-3} , 6.9×10^{-3} , 1.035×10^{-2} , 1.55×10^{-2} , 2.33×10^{-2} , 3.07×10^{-2} , and 4.52×10^{-2} M; cell path 1 cm. (B) Comparison of measured (open) and calculated (solid) circular dichroism variations (see text): (circle) 492 nm; (square) 460 nm. $T = 295$ K.

indicating the formation of inclusion complexes. In particular, the long-wavelength band undergoes a red shift ($\lambda_{\text{max}} = 466$ nm in the presence of $[\alpha\text{-CD}] = 2.1 \times 10^{-2}$ M and $\epsilon = 33.5$ M $^{-1}$ cm $^{-1}$; $\lambda_{\text{max}} = 460.5$ nm in the presence of $[\beta\text{-CD}] = 1.05 \times 10^{-2}$ M and $\epsilon = 34.5$ M $^{-1}$ cm $^{-1}$). The short-wavelength band loses intensity, and its vibronic structure becomes more manifest. The same behavior is displayed by the SCQ enantiomer.

Circular dichroism spectra nicely confirm the interactions between the camphorquinone enantiomers and the CDs. In Figures 2A and 3A, the spectra of RCQ and SCQ in water and in the presence of increasing α -CD concentrations are reported. The maxima fairly well correspond to those of the absorption spectra. RCQ in pure water has a negative structureless band peaked at 460 nm and a positive band centered at 300 nm in which five vibronic bands are clearly discernible. In the UV spectrum, these bands appear as shoulders of the second n, π^* band. The addition of increasing amounts of α -CD causes a red shift and a more intense signal of the negative band which now shows two maxima peaked at 472 and 486 nm. The positive

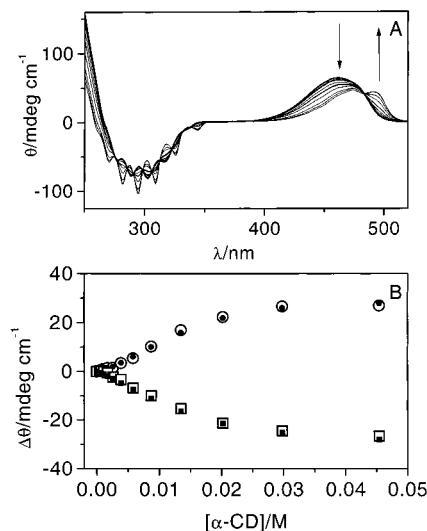


Figure 3. (A) Circular dichroism spectra of SCQ ($c = 4.77 \times 10^{-3}$ M) in water (—) and in the presence of increasing concentrations of α -CD (—); $[\alpha\text{-CD}] = 7.7 \times 10^{-4}$, 1.14×10^{-3} , 1.72×10^{-3} , 2.59×10^{-3} , 3.88×10^{-3} , 5.82×10^{-3} , 8.73×10^{-3} , 1.35×10^{-2} , 2.02×10^{-2} , 2.98×10^{-2} , and 4.54×10^{-2} M; cell 1 cm thick. (B) Comparison of measured (open) and calculated (solid) circular dichroism variations (see text): (circle) 492 nm; (square) 460 nm. $T = 295$ K.

band decreases in intensity, and the maximum of all of the vibronic bands undergoes a blue-shift (~ 3 nm). The spectral evolutions following the CD addition occur with isoelliptic points at ≈ 260 , 350, and 450 nm.

The SCQ enantiomer has a positive band peaked at 462 nm in water and a negative band, with vibrational structure, centered at 300 nm. In presence of α -CD, the positive band decreases in intensity, shifts to the red, and shows two maxima, at 471 and 494 nm. Owing to the α -CD addition, the UV band undergoes some intensity change (the signal becomes more negative), but the most remarkable effect is the red-shift (~ 7 nm) of the vibronic bands, as shown in Figure 3. These changes occur with isoelliptic points at 484 nm in the visible band and 337, 323, 313, 306, 298, 291, and 275 nm in the UV region.

The addition of β -, dimethyl- β -, and γ -CD to the aqueous solutions of the two enantiomers has a less spectacular effect: a small shift of the bands whose intensity is scarcely affected.

In conclusion, the induced icd signals appear similar in sign for the two CQ enantiomers and distinctly different for α -CD, on one side, and for β - and γ -CD, on the other side. Accordingly, in racemic CQ solutions, two negative bands are observed in the presence of α -CD, one in the UV, and one in the visible region, whereas the UV band is negative and the visible one is positive with the other CDs (Figure 4).

Racemic camphorquinone has fluorescence emission in air-saturated organic solvents at room temperature. The spectrum shows a vibronic structure ($\Delta\nu \approx 800$ cm $^{-1}$, solvent dependent), and the fluorescence quantum yield ($\Phi_f \approx 0.003$) does not depend on the polarity of the medium. Carefully purified samples show also, in oxygen-free solutions, phosphorescence emission, peaked at ~ 560 nm, with lifetime of hundreds microseconds, solvent dependent.²⁶

In water, the emission of both enantiomers is peaked at ~ 510 nm, a vibronic structure is hardly discernible, and the fluorescence yield is reduced to $\Phi_f \approx 0.0008$ (taking as reference $\Phi_f = 0.003$ in acetonitrile²⁶). No phosphorescence emission could be observed even after prolonged deaeration by bubbling with pure nitrogen. Double recrystallization of the RCQ enantiomer from cyclohexane did not modify the emission characteristics

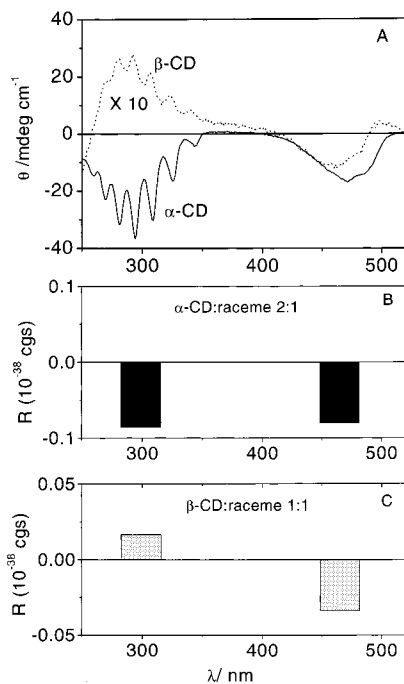


Figure 4. (A) Circular dichroism spectra of 4.5×10^{-3} M camphorquinone racemate, induced by 1.03×10^{-2} M α -CD (—) and 1.07×10^{-2} M β -CD (---), at 295 K; computed icd for the α -CD:CQ racemate 2:1 complex (B) and for the β -CD:CQ racemate 1:1 complex.

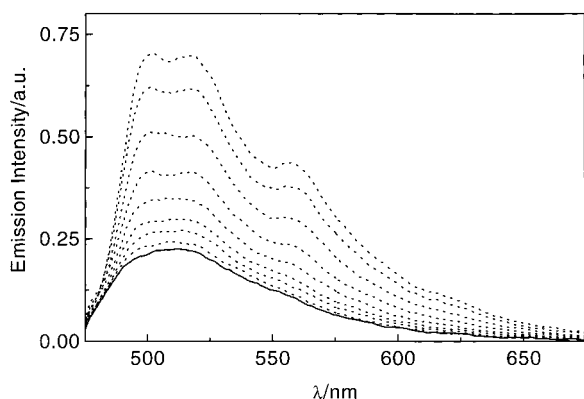


Figure 5. Emission spectrum of SCQ ($c = 1.55 \times 10^{-3}$ M) in water (—) and in the presence of increasing concentrations of α -CD (···). $[\alpha\text{-CD}] = 8 \times 10^{-4}$, 1.8×10^{-3} , 2.7×10^{-3} , 4.05×10^{-3} , 6.07×10^{-3} , 9.11×10^{-3} , 1.37×10^{-2} , and 2.05×10^{-2} M. $T = 295$ K.

in water. The addition of cyclodextrins to water solutions of the two enantiomers greatly increased (2–3 times) the overall emission and, when α -CD is used as host, modified the spectral distribution. An example of the described effects is reported in Figures 5 and 6 which show the variations of the emission yield of the SCQ enantiomer as a function of $[\alpha\text{-CD}]$ and $[\beta\text{-CD}]$, respectively. In general, a vibronic structure is more clearly discernible in the presence of all of the cyclodextrins, and when α -CD is the host, a band peaked at ~ 560 nm increases with increasing $[\alpha\text{-CD}]$. This band should be attributed to the phosphorescence emission.²⁶

Complexation Equilibria. The stoichiometry of the complexation and the values of the association constants between the two camphorquinone enantiomers and the cyclodextrins were determined by a combination of icd, absorption, and fluorescence measurements. At first, the observed variations of the ellipticity ($\Delta\theta$), induced by the presence of cyclodextrins, were examined according to the method of the continuous variations.²⁷ For both enantiomers, the greatest signal variation was observed

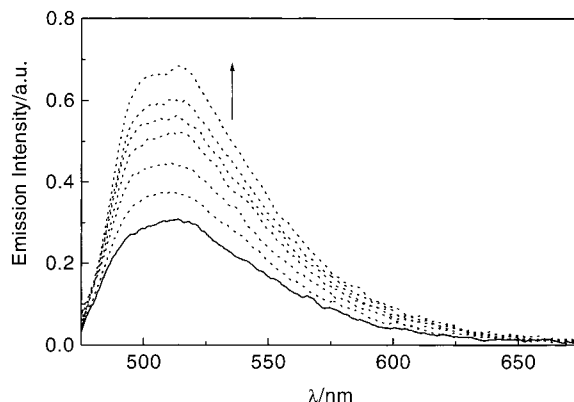


Figure 6. Emission spectrum of SCQ ($c = 1.58 \times 10^{-3}$ M) in water (—) and in the presence of increasing concentrations of β -CD (···). $[\beta\text{-CD}] = 7.84 \times 10^{-4}$, 1.77×10^{-3} , 3.00×10^{-3} , 3.92×10^{-3} , 5.11×10^{-3} , and 1.13×10^{-2} M. $T = 295$ K.

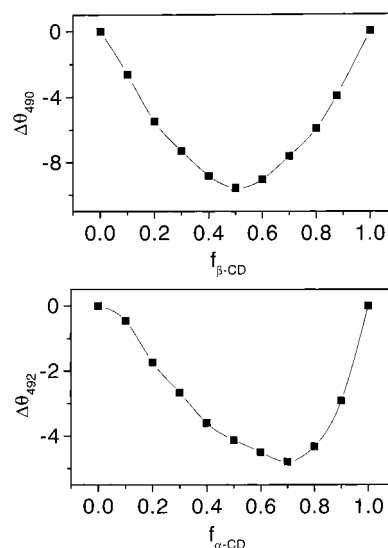


Figure 7. Continuous variation curves for the circular dichroism of 4.65×10^{-3} M RCQ in the presence of β -CD (A) and α -CD (B). $T = 295$ K.

for molar fraction 0.5 with all of the cyclodextrins, except α -CD. This indicates a 1:1 stoichiometry for the formed complex. The corresponding curves for the variations induced by the α -CD both in the short and in the long-wavelength band gave a maximum at molar fraction ~ 0.7 , which indicates that, in the adopted experimental conditions, the $\Delta\theta$ values are due to a 2:1 (host/guest) stoichiometry of the complex. An example of the obtained continuous variation curves for the interaction of RCQ and α - and β -CD is reported in Figure 7.

The fluorescence intensity was employed to determine the values of the equilibrium constants in the presence of β -CD, dimethyl- β -, and γ -CD. As an example, in Figure 8A, the values of the ratio F/F_0 (ratio between the integrated emission in the presence and that in absence of CD) are reported as a function of $[\beta\text{-CD}]$ for the SCQ enantiomer. The emission changes for the other CDs and for RCQ (not shown for the sake of brevity) are similar. They are consistent with the exclusive formation of a 1:1 complex. The determination of the association constants K_1 can be achieved assuming that the ground-state complexation equilibrium is not perturbed in the excited singlet state. This hypothesis is reasonable because the singlet lifetime is of the order of a few nanoseconds²⁶ and the dissociation of such kind of inclusion complexes is expected to occur on the microsecond time scale.^{1,12,19,28,29} The following equation holds for the

TABLE 1: Association Constants of Camphorquinone Enantiomers with α -, β -, γ -, and $(\text{CH}_3)_2\text{-}\beta$ -CD in Water at 295 K^a

	<i>R</i> -(-)-camphorquinone			<i>S</i> -(+)-camphorquinone		
	K_1/M^{-1}	K_2/M^{-1}	K_3/M^{-2}	K_1/M^{-1}	K_2/M^{-1}	K_3/M^{-2}
α -CD			7300 ± 600 (6500 ± 850) eq 9	22 ± 5		14100 ± 1700 (12400 ± 1750) eq 9
β -CD	510 ± 60			320 ± 15		
γ -CD	460 ± 30			430 ± 20		
$(\text{CH}_3)_2\text{-}\beta$ -CD	630 ± 50			440 ± 20		

^a The K_i values were obtained by best fitting of the experimental emission ratio F/F_0 to eq 4, except in the case of α -CD where icd data were analyzed via an iterative numerical procedure (see text); values in parentheses were obtained by applying eq 9 to absorption data. Errors given are mathematical uncertainties (two times the standard deviation of the optimized parameters, suitably rounded).

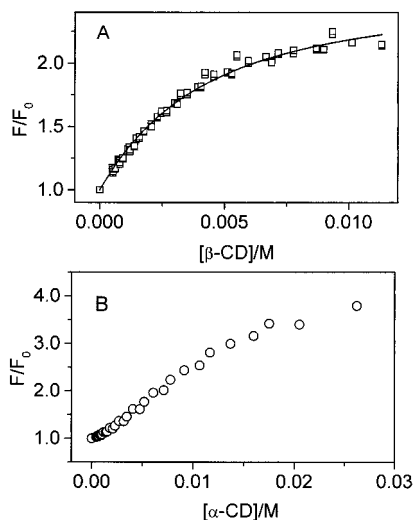


Figure 8. Dependence of the SCQ (1.55×10^{-3} M) integrated emission intensity ratio F/F_0 : (A) on $[\beta\text{-CD}]$ and (B) on $[\alpha\text{-CD}]$. $T = 295$ K, $\lambda_{\text{exc}} = 455$ nm, isosbestic point of the CD-containing solutions. The continuous line in (A) represents the best fit to eqs 4 with parameters $K_1 = 317 \text{ M}^{-1}$ and $\varphi_1/\varphi_0 = 2.6$.

integrated emission ratio F/F_0 of a solution of CQ (initial concentration $[\text{CQ}]_0$) in the presence of CD (initial concentration $[\text{CD}]_0$):

$$F/F_0 = 1 + (\varphi_1 - \varphi_0)[\text{CQ}\cdot\text{CD}]/(\varphi_0[\text{CQ}]_0) \quad (4)$$

where φ_0 and φ_1 stand for the fluorescence quantum yields of the free CQ and the 1:1 CD·CQ complex, respectively. The concentration of the complex is exactly expressed by eq 5:

$$[\text{CQ}\cdot\text{CD}] = (2K_1)^{-1}(K_1[\text{CQ}]_0 + K_1[\text{CD}]_0 + 1 - ((K_1[\text{CQ}]_0 + K_1[\text{CD}]_0 + 1)^2 - 4K_1^2[\text{CQ}]_0[\text{CD}]_0)^{0.5}) \quad (5)$$

The values of K_1 at 295 K for RCQ and SCQ and β -CD, dimethyl- β -, and γ -CD, obtained by a nonlinear least-squares fitting procedure of the experimental F/F_0 values according to eqs 4 and 5, are collected in Table 1. The reported values are the mean of three to four independent runs of the emission intensity versus the cyclodextrin concentration. Using the intensities at the maximum wavelength of the fluorescence spectra instead of the integrated emission F gave essentially the same results.

The dependence of the ratio F/F_0 on the α -CD concentration (Figure 8B) confirms the indication of the continuous variation plot that the complexation stoichiometry is higher than 1:1. In view of the theoretical calculations (see below) and the icd results, the interaction between the two enantiomers and α -CD can be discussed on the basis of a model of sequential formation

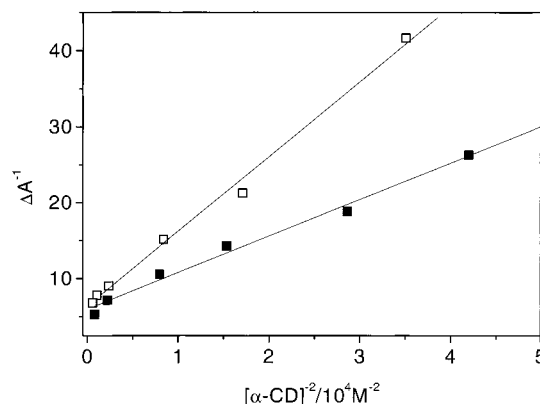
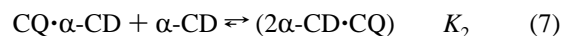


Figure 9. Benesi–Hildebrand-type plot for the variation of the absorption spectra in the complexation between $[\text{RCQ}] = 1.96 \times 10^{-3}$ M (\square) and $[\text{SCQ}] = 1.99 \times 10^{-3}$ M (\blacksquare) and two molecules of α -CD at 295 K. Cell path 4 cm.

of 1:1 and 2:1 host–guest complexes. The following equilibria are considered:



On the other hand, the continuous variations plot of the icd signal (Figure 7) suggests that the complexation equilibrium can be also approximated by the simultaneous association of two α -CD molecules to a camphorquinone molecule (eq 8):



To roughly estimate K_3 , we first used a Benesi–Hildebrand-like analysis of the ground-state absorption data in the range of 482–496 nm, where the first $n,\pi^* \leftarrow n,\pi$ transition is strongly enhanced by α -CD complexation (see Figure 1), and the following equation:

$$1/\Delta A = \text{Cost}(1 + 1/(K_3[\alpha\text{-CD}]_0^2)) \quad (9)$$

where ΔA is the absorbance change measured as a function of α -CD concentration, K_3 corresponds to the product K_1K_2 of the association constants in the equilibria (6) and (7), and Cost is a constant related to the molar absorption coefficients of the free and the complexed guest. This equation requires that $[\alpha\text{-CD}]_0$ is in large excess over $[\text{CQ}]_0$. This condition is hardly fulfilled with CQ because of the low absorption coefficients. Thus, absorption data were generated with $[\text{CQ}]_0 \sim 0.002$ M, a concentration lower, but not much lower, than that adopted for the host, $0.005 < [\alpha\text{-CD}]_0 < 0.05$ M. The plots $1/\Delta A$ vs $1/[\alpha\text{-CD}]_0^2$ for RCQ and SCQ exhibit a good linearity (Figure 9). The recovered values for the slope/intercept ratio, 6500 M^{-2} for RCQ and $12\,400 \text{ M}^{-2}$ for SCQ, although questionable as

TABLE 2: Stoichiometry, Number of Low Energy Configurations, and Energetic Characterization of Enantiomeric Camphorquinone-CD Complexes in Water

complex	stoichiometry	no. of configurations	$\Delta E_p/$ kJ mol ^{-1a}	$\Delta E_c/$ kJ mol ^{-1a}
α :RCQ	1:1	541	-47.4	-20.1
	2:1	200	-251.6	-78.0
α :SCQ	1:1	650	-75.4	-50.2
	2:1	152	-262.9	-90.6
β :RCQ	1:1	653	-100.1	-84.9
β :SCQ	1:1	647	-96.7	-77.8
γ :RCQ	1:1	667	-118.2	-69.8
γ :SCQ	1:1	650	-123.2	-76.4

^a ΔE_p gives the potential energy of complexation. ΔE_c gives the total complexation energy. For the definition of these quantities, see the text in the Conformation of the Complexes section.

binding constants K_3 (they are therefore indicated in parentheses in Table 1), point to a difference in the binding ability of α -CD toward the two enantiomers. This result was confirmed by the analysis of the data of icd titration experiments, employing the computer program Hyperquad 2000,¹⁸ which afforded association constants by a least-squares minimization procedure. The calculation essentially consisted in the minimization of the following quantity:

$$S = \sum_{i=1}^m \left(\frac{\Delta\theta_i^{\text{obs}} - \Delta\theta_i^{\text{calc}}}{\Delta\theta_i^{\text{obs}}} \right)^2 \quad (10)$$

representing the sum of the squared residues resulting from the comparison of measured with calculated values of the total induced ellipticity between 520 and 380 nm (141 wavelengths) at a number (from 10 to 13) concentrations of α -CD, with each species in solution contributing with its own spectrum and proportionally to its concentration. Two models were assumed for the association, i.e., a sequential 1:1 plus 1:2 complexation or the exclusive formation of 1:2 complexes. For the *S* enantiomer, the calculation afforded $K_1 = 22 \text{ M}^{-1}$ and $K_3 = 14\,100 \text{ M}^{-2}$. With the *R* enantiomer, no convergence was obtained with the two-complex model. By assuming exclusive formation of the 1:2 complex, the value $K_3 = 7300 \text{ M}^{-1}$ was obtained. In Figures 2B and 3B, the measured and calculated ellipticity variations are represented for the *R* and *S* enantiomers, respectively.

Conformation of the Complexes. The calculations fully confirm the found stoichiometry of the complexes and furnish their structures. The search for minimum energy structures gave rise to a large number of accepted configurations (~ 600) for the 1:1 complexes independently of the type of macrocycle considered, with potential energies ranging from 397 to 439 kJ/mol⁻¹. On the other hand a reliable 2:1 stoichiometry was found only for the complex formed in α -CD, with a much lower number of accepted configurations (150–200) at 464–478 kJ/mol⁻¹, and with the SCQ enantiomer being favored for inclusion with respect to RCQ (see Table 2). A typical pattern of low energy structures pointing out the structural differences of the formed complexes is displayed in Figure 10A–D. The CQ molecules are deeply included in the γ -CD cavity and quite peripherally in that of β -CD. In the complex with β -CD, the more lipophilic part of the molecule is embedded in the cavity, whereas the two carbonyl groups are in proximity of the secondary hydroxyls rim. Last, in the 1:1 complex with α -CD, the chromophore tends to stay well outside the cavity (Figure 10A), and the intervention of another α -CD confines the guest in the low energy structure shown in Figure 10B. These two

structures well explain why the continuous variation plot of the circular dichroism signal induced by α -CD is dominated by the 2:1 complex (vide supra); likely the “external” location of the guest in the 1:1 complex causes only a minor perturbation of the intrinsically high circular dichroism signal of the two CQ enantiomers, whereas the interaction becomes strong when the second α -CD blocks the molecule in the structure of Figure 10B.

In Table 2, ΔE_p gives the difference in potential energy comparing the potential energy of a typical low energy complex with the sum of the potential energies of isolated host and guest. ΔE_c gives the total complexation energy considering both potential as well as solvation energy. ΔE_c is computed as the difference between sum of the potential and solvation energy of the complex and sum of the potential and solvation energy of the respective isolated compounds. The energetic parameters of the isolated compounds are (given as pairs of potential and solvation energy in kJ mol⁻¹) α -CD (257.3 and -186.6), β -CD (298.3 and -210.5), γ -CD (346.1 and -236.7), and CQ (214.8 and -16.2). The difference in the potential energies of complexation of the two CQ enantiomers and α -CD nicely parallels the difference observed in the association constants. The same difference is reproduced in the total complexation energies. On the contrary, the difference in the potential energies of complexation of the two CQ enantiomers in the larger β - and γ -CD cavities are smaller than those found in the total energy of complexation. This result indicates that solvation terms contribute strongly to chiral recognition in more loose complexes, whereas the host/guest interaction is mainly responsible for chiral discrimination in well defined, tight structures.

The reliability of the above conformations was tested by calculating the induced circular dichroism and comparing it with the experimental signals obtained from the racemate. This procedure overcomes the difficulty to reproduce the intrinsic signal of the pure enantiomers, which is extremely sensitive to tiny conformational features and requires the treatment of localized electronic transitions and/or intramolecular charge transfer configurations, not properly described within the used computational framework. Figure 4 reports the icd spectrum of the racemate in the presence of 10^{-2} M α - and β -CD (Figure 4A) and the calculated icd (Figure 4B and 4C) for an average of the accepted configurations. The correct sign of the calculated icd (i.e., two negative bands) was given by about 20 configurations for the α -CD complex with 2:1 stoichiometry, whereas no one was given for the 1:1 stoichiometry. On the other hand, almost all of the accepted configurations for the β -CD complex (653) gave rise to a correct pattern of positive and negative bands. In conclusion, the icd calculations support the idea of a multiple stoichiometry for the α -CD complex and of 1:1 complexation for the two larger cyclodextrins.

Transient Absorption. Laser excitation at 460 nm of aqueous solutions of both RCQ and SCQ (typically $5.5 \times 10^{-3} \text{ M}$) leads to the formation of a long-lived transient identified as the lowest triplet state of n,π^* character.³⁰ The difference spectrum of RCQ taken 0.6 μs after the laser pulse, shown in Figure 11, with λ_{max} at 300–310 nm and decay in the microsecond time domain is indeed attributed to T–T absorption in agreement with the literature data.³¹ The lifetime in oxygen-free aqueous solutions ($\tau_0 \sim 20 \mu\text{s}$) is 1 order of magnitude shorter than that previously reported and derived from phosphorescence decay measurements in various non-H-bonding donor solvents (200–400 μs).²⁶ Such a shortening could be related to concentration (self-quenching) or excitation intensity effects, although we can hypothesize that specific interactions of the carbonyl groups with water molecules

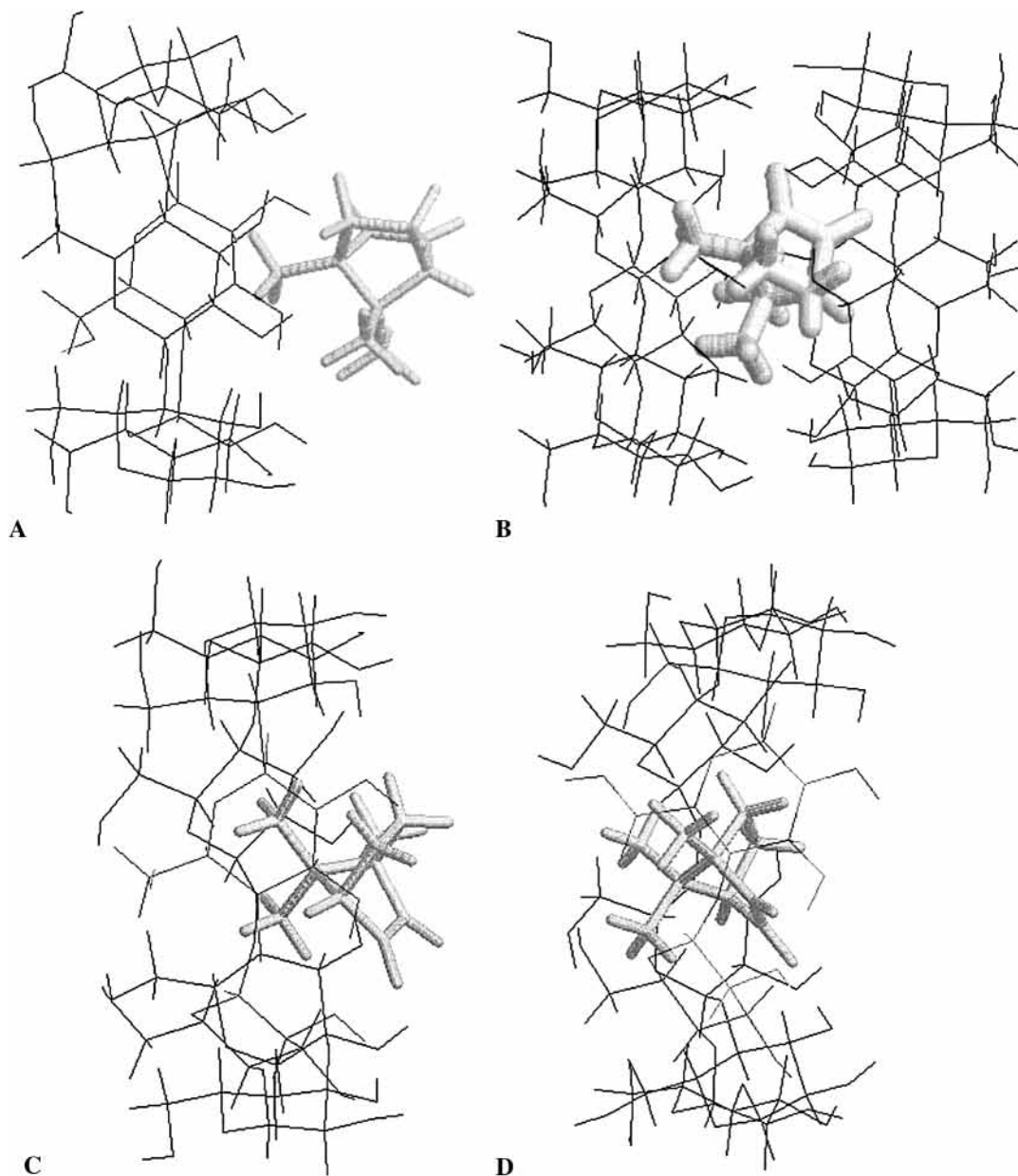


Figure 10. Computed conformation of the (A) 1:1 complex with α -CD, (B) 2:1 complex with α -CD, (C) 1:1 complex with β -CD, and (D) 1:1 complex with γ -CD.

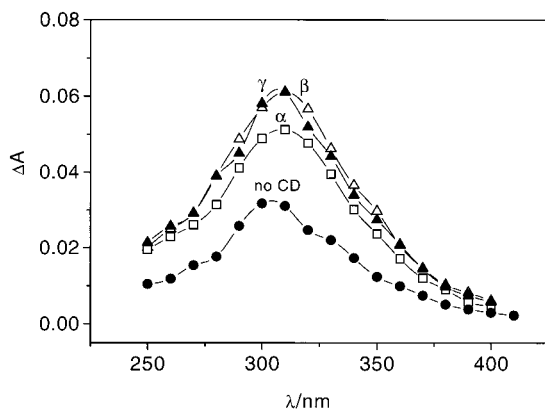


Figure 11. Transient absorption spectra of 5.5×10^{-3} M RCQ in water and in the presence of 1×10^{-2} M α -CD (\bullet), β -CD (Δ), and γ -CD (\blacktriangle). $\lambda_{\text{exc}} = 460$ nm, cell path 1 cm, $T = 295$ K.

may play some role. In agreement with such a hypothesis, the efficiency of the ISC process in aqueous medium is not unitary

(see below) in contrast to what is generally assumed to be valid in both polar and apolar solvents.²⁶ The decay rate ($k_0 = 5 \times 10^4 \text{ s}^{-1}$) was moderately affected by oxygen, ($k_{\text{O}_2} = 3.5 \times 10^8 \text{ M}^{-1} \text{ s}^{-1}$) as reported for the n,π^* triplet of camphorquinone and other α -diketones in different organic solvents.³² A τ value of $7 \pm 1 \mu\text{s}$, the same for both of the enantiomers, was extracted from the exponential treatment of the decay profiles at 310 nm in air equilibrated solutions (Figure 12A,B).

In presence of 1.0×10^{-2} M α -CD, the triplet decay was biexponential with $\tau_1^{\alpha\text{R}} = 5 \pm 1 \mu\text{s}$ and $\tau_2^{\alpha\text{R}} = 45 \pm 5 \mu\text{s}$ (Figure 12a). The relative weight of the two components varied with the α -CD concentration, with the longer-lived one becoming heavier and heavier as the CD concentration increases. Similar results were obtained with SCQ for which $\tau_1^{\alpha\text{S}} = 4 \pm 1 \mu\text{s}$ and $\tau_2^{\alpha\text{S}} = 55 \pm 5 \mu\text{s}$ (Figure 12b). In presence of 1×10^{-2} M β -CD, the triplet decay profiles of the RCQ enantiomer are also compatible with a biexponential function, with the second lifetime considerably lengthened with respect to that in pure water ($\tau_1^{\beta\text{R}} = 5 \pm 2 \mu\text{s}$ and $\tau_2^{\beta\text{R}} = 35 \pm 5 \mu\text{s}$). With $1 \times$

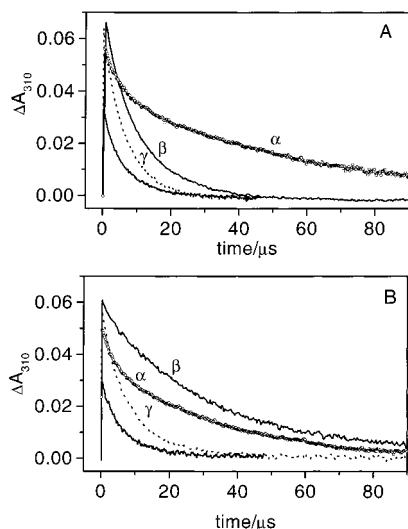


Figure 12. T–T absorption decay of air saturated SCQ (A) and RCQ (B) solutions in water and in the presence of 1×10^{-2} M α -, β -, and γ -CD. $[RCQ] = [SCQ] = 5.5 \times 10^{-3}$ M; $\lambda_{exc} = 460$ nm, cell path 1 cm, $T = 295$ K.

TABLE 3: Triplet Lifetimes of Camphorquinone Enantiomers in the Presence of α -, β -, and γ -CD in Water at 295 K

	<i>R</i> (-)-camphorquinone triplet lifetime		<i>S</i> (+)-camphorquinone triplet lifetime	
	$\tau_1/\mu\text{s}$	$\tau_2/\mu\text{s}$	$\tau_1/\mu\text{s}$	$\tau_2/\mu\text{s}$
H ₂ O	6.7 ± 1		7.0 ± 1	
10^{-2} M α -CD	5 ± 1	45 ± 5	4 ± 1	55 ± 5
10^{-2} M β -CD	5 ± 2	35 ± 5	11 ± 1	
10^{-2} M γ -CD	8 ± 1		7 ± 1	

10^{-2} M β -CD and the SCQ enantiomer and with 1×10^{-2} M γ -CD and both enantiomers, the best fits of the triplet decay profiles are not expressed by multiple components but appear monoexponential with lifetimes only slightly changed ($\tau^{\beta S} = 11 \pm 1 \mu\text{s}$, $\tau^{\gamma R} = 8 \pm 1 \mu\text{s}$, and $\tau^{\gamma S} = 7 \pm 1 \mu\text{s}$). All of the triplet lifetimes are collected in Table 3 for the sake of clarity.

The biexponential triplet decay of RCQ and SCQ enantiomers in the presence of α -CD can be interpreted in the light of the complexation equilibria. The short-lived component, very similar to that in pure water, is reasonably assigned to the free guest and/or to the 1:1 complex which is characterized by a very peripheral association mode (Figure 10A). The long-lived component is attributed to the 2:1 complex, in which effective protection of the excited state from the aqueous environment occurs. This seems to apply to the rather long-lived β -CD·RCQ 1:1 triplet complex also. Unexpectedly, the β -CD·SCQ 1:1 diastereoisomer shows a lifetime only slightly changed with respect to that of the pure enantiomer in water. A possible rationale for this fact could be the existence of a lower association constant for the triplet SCQ than for the triplet RCQ, similarly to the ground-state findings. In this case, the exit of the excited state from the cavity should occur at a rate fast enough to be compatible with the observed overall decay rate ($\sim 10^5 \text{ s}^{-1}$). The values reported in the literature, ca. 10^6 s^{-1} ,^{1,12,19,28,29} are not in contrast with this hypothesis.

The lack of effect of γ -CD inclusion on the triplet lifetimes of both RCQ and SCQ could be similarly attributed to prompt dissociation of the complexes prior to triplet deactivation, so that no differences are observed in the two diastereoisomers. The alternative explanation that included water molecules could make the cavity environment substantially hydrophilic is rejected in view of the effect on the Φ_T discussed in the following.

The addition of 1×10^{-2} M CD to RCQ and SCQ solutions sensibly increases (by a factor 1.6–2) the T–T absorption following the laser pulse at 460 nm, which is the isosbestic point of the camphorquinone-cyclodextrin solutions (see Figure 11). This effect is properly quantified by taking into account that CQ absorbs light in the range of 250–400 nm and ground-state bleaching occurs. The differential absorption is expressed by

$$\Delta A = (\epsilon_T - \epsilon_G)l[CQ]_T \quad (11)$$

where ϵ_T and ϵ_G are the absorption coefficients of the triplet and the ground-state, respectively, l is the cell path, and $[CQ]_T$ gives the triplet molar concentration. The triplet signal in both the absence and presence of CDs can thus be obtained from ΔA , being the ϵ_G values known from the ground-state absorption and the triplet concentration calculated by taking $\Phi_T = 1$ for both free and complexed CQ.²⁶ The additive corrections to ΔA for $\lambda \geq 270$ nm are in any case $< 10\%$; thus, the enhancement observed in the presence of CDs cannot be attributed to a smaller ground state bleaching term. Because the band profile is practically unchanged, the ϵ_T values are not expected to be strongly increased by CD addition, and necessarily, $[CQ]_T$ should be increased. By taking into account the extent of association in the experiment (30–35% with α - and ca. 70% with β - and γ -CD for both RCQ and SCQ, either in the 1:1 or in the 2:1 mode, see Table 1), it is concluded that Φ_T in the CD complexes is higher than in water by more than a factor 2. With the fluorescence quantum yield of CQ enantiomers being rather low ($\sim 10^{-3}$), these findings indicate that in water non radiative channels other than ISC contribute to deactivation of the excited singlet, so that the Φ_T value is substantially less than 1 and that such channels are closed in the CD environment. It is noteworthy that in mixed ethanol–water solvent the T–T absorption of both CQ enantiomers also increases with increasing ethanol percentages. This fact could point to an interaction of the alcoholic CD rims with the camphorquinone carbonyl groups.

Chiral Discrimination. The equilibrium constants collected in Table 1 and, in part, the triplet lifetimes indicate a distinct chiral discrimination of cyclodextrins toward the two camphorquinone enantiomers. (*1R*)(-)-Camphorquinone is preferentially included by cyclodextrins which gives only 1:1 host/guest complexes (β -, dimethyl- β -, and γ -CD), whereas (*1S*)(+)-camphorquinone is preferentially included in the 2:1 complex with α -CD. A similar discrimination of α -CD was already observed by NMR in the complexation of the camphor enantiomers.¹⁴ On the basis of the association constants reported in Table 1, in 1:1 complexes the differences in ΔG values ($\Delta\Delta G$) between RCQ and SCQ are in the range 0.2–1.2 kJ mol⁻¹ as in most cases in the literature.³³ In the complexes between the two camphorquinone enantiomers and α -CD, the $\Delta\Delta G$ increases to ~ 1.9 kJ mol⁻¹, i.e., somewhat higher than the difference found for the complexes between camphor enantiomers and α -CD.¹⁴ Reasonably, this increase in chiral recognition ability is related to the formation of 2:1 complexes. Complexation of enantiomeric binaphthyl derivatives are the examples of largest selectivity reported with cyclodextrins which give 1:1 stoichiometries (β -, dimethyl- β -, and trimethyl- β -CD).¹⁰ In these cases, the selectivity rises from a positive entropic contribution attributed to extensive desolvation of both the guest and the oxygen of the wider side of the CD cavity. On the other hand, a study of chiral recognition by β -CD on the nitrophenyl derivatives of L- and D-valine, leucine, and methionine^{33d} suggests that the interaction of functional groups around the chiral center

with the mouth of the cavity and/or another CD (i.e., the formation of a 2:1 complex) is an essential requirement to observe chiral discrimination. The latter model fits well the observed behavior of camphor and camphorquinone enantiomers. Indeed the calculated energetics of complexation for the diastereoisomeric α -CD•CQ complexes points to a crucial role of enthalpic factors in the stability of these associates. However, a contribution of the desolvation processes cannot be excluded, especially for β - and γ -CD•CQ complexes where the entropic factors are expected to be more important.

Acknowledgment. We thank dr. Francesco Barigelletti for helpful discussions in the use of the Hyperquad 2000 computer program.

References and Notes

- (1) (a) Bender, M. L.; Komiyama, M. *Cyclodextrin Chemistry*; Springer-Verlag: Berlin, 1978. (b) Szejtli, J. *Cyclodextrins and Their Inclusion Complexes*; Akademiai Kiado: Budapest, Hungary, 1982. (c) Clarke, R. J.; Coates, J. H.; Lincoln, S. F. *Adv. Carbohydr. Chem. Biochem.* **1989**, *46*, 205.
- (2) Sensse, K.; Cramer, F. *Chem. Ber.* **1969**, *102*, 509.
- (3) (a) Hinze, W. L.; Riehl, T. E.; Armstrong, D. W.; DeMond, W.; Alak, A.; Ward, T. *Anal. Chem.* **1985**, *57*, 237. (b) Schurig, V.; Nowotny, H.-P. *Angew. Chem., Int. Ed. Engl.* **1990**, *29*, 939. (c) Li, S.; Purdy, W. C. *Chem. Rev.* **1992**, *92*, 1457. (d) Kuhn, K.; Hoffstetter-Kuhn, S. *Chromatographia* **1992**, *34*, 505. (e) Wistuba, D.; Schurig, V. *J. Chromat.* **2000**, *875*, 255. (f) Ward, T. *J. Anal. Chem.* **2000**, *72*, 4521.
- (4) (a) Kano, K.; Matsumoto, K.; Hashimoto, S.; Sisido, M.; Imanishi, Y. *J. Am. Chem. Soc.* **1985**, *107*, 6117. (b) Kano, K.; Matsumoto, H.; Yoshiyasu, Y.; Hashimoto, S. *J. Am. Chem. Soc.* **1988**, *110*, 204.
- (5) LeBas, G.; de Rango, C.; Rysanek, N.; Tsoucaris, G. *J. Incl. Phenom.* **1984**, *2*, 861.
- (6) Kano, K.; Yoshiyasu, K.; Hashimoto, S. *J. Chem. Soc., Chem. Commun.* **1989**, 1278.
- (7) Brown, S. E.; Coates, J. H.; Duckworth, P. A.; Lincoln, S. F.; Easton, C. J.; May, B. L. *J. Chem. Soc. Faraday Trans.* **1993**, *89*, 1035.
- (8) Brown, S. E.; Haskard, C. A.; Easton, C. J.; Lincoln, S. F. *J. Chem. Soc. Faraday Trans.* **1995**, *91*, 1013.
- (9) Rekharsky, M. V.; Goldberg, R. N.; Schwarz, F. P.; Tewari, Y. B.; Ross, P. D.; Yamashoji, Y.; Inoue, Y. *J. Am. Chem. Soc.* **1995**, *117*, 8830.
- (10) Kano, K.; Kato, Y.; Kodera, M. *J. Chem. Soc., Perkin Trans. 2* **1996**, 1211.
- (11) Kano, K. *J. Phys. Org. Chem.* **1997**, *10*, 286.
- (12) Barros, T. C.; Stefaniak, K.; Holzwarth, J. F.; Bohne, C. *J. Phys. Chem. A* **1998**, *102*, 5639.
- (13) Kano, K.; Kamo, H.; Negi, S.; Kitae, T.; Takaoka, R.; Yamaguchi, M.; Okubo, H.; Hiramata, M. *J. Chem. Soc., Perkin Trans. 2* **1999**, 15.
- (14) Dodziuk, H.; Ejchart, A.; Lukin, O.; Vysotsky, M. O. *J. Org. Chem.* **1999**, *64*, 1503.
- (15) Easton, C. J.; Lincoln, S. F. *Chem. Soc. Rev.* **1996**, 163.
- (16) (a) Grabner, G.; Monti, S.; Marconi, G.; Mayer, B.; Klein, Ch. Th.; Köhler, G. *J. Phys. Chem.* **1996**, *100*, 20069. (b) Murphy, R. S.; Barros, T. C.; Mayer, B.; Marconi, G.; Bohne, C. *Langmuir* **2000**, *16*, 8780. (c) Mayer, B.; Marconi, G.; Klein, C. T.; Koehler, G. *J. Incl. Phenom. Mol. Recogn. Chem.* **1997**, *29*, 79.
- (17) (a) Monti, S.; Köhler, G.; Grabner, G. *J. Phys. Chem.* **1993**, *97*, 13011. (b) Bortolus, P.; Marconi, G.; Monti, S.; Mayer, B.; Koehler, G.; Grabner, G. *Chem. Eur. J.* **2000**, *6*, 1578. (c) Bortolus, P.; Marconi, G.; Monti, S.; Grabner, G.; Mayer, B. *Phys. Chem. Chem. Phys.* **2000**, *2*, 2943.
- (18) Alderighi, L.; Gans, P.; Ienco, A.; Peters, D.; Sabatini, A.; Vacca, A. *Coord. Chem. Rev.* **1999**, *184*, 311.
- (19) (a) Monti, S.; Flamigni, L.; Martelli, A.; Bortolus, P. *J. Phys. Chem.* **1988**, *92*, 4447. (b) Monti, S.; Camaioni, N.; Bortolus, P. *Photochem. Photobiol.* **1991**, *54*, 577.
- (20) Schellman, J. A. *Acc. Chem. Res.* **1968**, *1*, 4927.
- (21) Woody, R.; Tinoco, I., Jr. *J. Chem. Phys.* **1967**, *46*, 4927.
- (22) Tinoco, I., Jr. *Adv. Chem. Phys.* **1962**, *4*, 113.
- (23) Hezemans, A. M. F.; Obbink, J. H. *Theor. Chem. Acta* **1976**, *43*, 75.
- (24) Hug, W.; Wagnière, G. *Helv. Chim. Acta* **1971**, *54*, 633. (b) Hug, W.; Kuhn, J.; Seibold, K. J.; Labhart, H.; Wagnière, G. *Helv. Chim. Acta* **1971**, *54*, 1451.
- (25) Verheijdt, P. L.; Cerfontain, H. *J. Chem. Soc. Perkin Trans. 2* **1982**, 1541.
- (26) (a) Romani, A.; Favaro, G.; Masetti, F. *J. Lumin.* **1995**, *63*, 183. (b) Favaro, G.; Malatesta, V.; Miliari, C.; Romani, A. *J. Photochem. Photobiol. A: Chem.* **1996**, *97*, 45.
- (27) (a) Beck, M. T. *Chemistry of Complex Equilibria*; Van Nostrand: New York, 1970. (b) Connors, K. A. *Binding Constants—The Measurement of Molecular Complex Stability*; John Wiley & Sons: New York, 1987.
- (28) Barra, M.; Bohne, C.; Scaiano, J. C. *J. Am. Chem. Soc.* **1990**, *112*, 8075.
- (29) Liao, Y.; Bohne, C. *J. Phys. Chem.* **1996**, *100*, 734.
- (30) A further transient was observed, absorbing around 300–320 nm, with a lifetime of ca. 10 ns. A tentative assignment of this absorption to the lowest n,π^* singlet state is in agreement with time-resolved fluorescence decay by single photon counting.
- (31) Nau, W.; Scaiano, J. C. *J. Phys. Chem.* **1996**, *100*, 11360.
- (32) Darmanyan, A. P.; Foote, C. S.; Jardon, P. J. *J. Phys. Chem.* **1995**, *99*, 11854.
- (33) (a) Cooper, A.; MacNicol, D. D. *J. Chem. Soc. Perkin Trans. 2* **1978**, 760. (b) Ihara, Y.; Nakanishi, E.; Nango, M.; Koga, J. *Bull. Chem. Soc. Jpn.* **1986**, *59*, 1901. (c) Brown, S. E.; Coates, J. H.; Lincoln, S. F.; Coghlan, D. R.; Easton, C. J. *J. Chem. Soc. Faraday Trans.* **1991**, *87*, 2699. (d) Li, S.; Purdy, W. C. *Anal. Chem.* **1992**, *64*, 1405. (e) Feibush, B.; Woolley, C. L.; Mami, V. *Anal. Chem.* **1993**, *65*, 1130. (f) Rekharsky, M. V.; Inoue, Y. *Chem. Rev.* **1998**, *98*, 1875.